



CANCER DISCOVERY

Genomic Complexity and AKT Dependence in Serous Ovarian Cancer

Aphrothiti J. Hanrahan, Nikolaus Schultz, Maggie L. Westfal, et al.

Cancer Discovery 2012;2:56-67. Published OnlineFirst November 3, 2011.

Updated version	Access the most recent version of this article at: doi:10.1158/2159-8290.CD-11-0170
Supplementary Material	Access the most recent supplemental material at: http://cancerdiscovery.aacrjournals.org/content/suppl/2011/11/03/2159-8290.CD-11-0170.DC2.html

Cited Articles This article cites by 47 articles, 15 of which you can access for free at:
<http://cancerdiscovery.aacrjournals.org/content/2/1/56.full.html#ref-list-1>

Citing articles This article has been cited by 2 HighWire-hosted articles. Access the articles at:
<http://cancerdiscovery.aacrjournals.org/content/2/1/56.full.html#related-urls>

E-mail alerts [Sign up to receive free email-alerts](#) related to this article or journal.

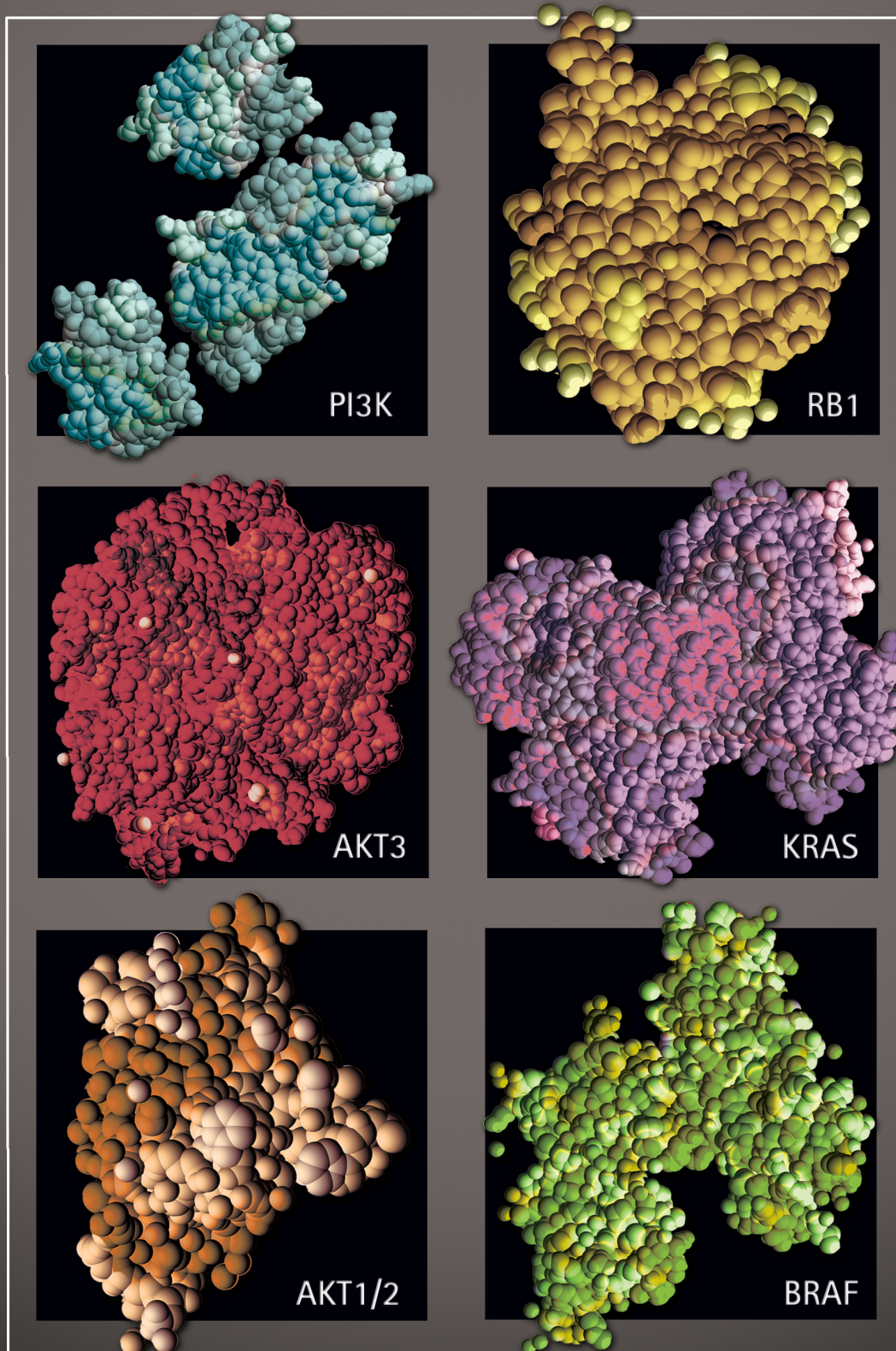
Reprints and Subscriptions To order reprints of this article or to subscribe to the journal, contact the AACR Publications Department at pubs@aacr.org.

Permissions To request permission to re-use all or part of this article, contact the AACR Publications Department at permissions@aacr.org.

RESEARCH ARTICLE

Genomic Complexity and AKT Dependence in Serous Ovarian Cancer

Aphrothiti J. Hanrahan¹, Nikolaus Schultz², Maggie L. Westfall¹, Rita A. Sakr³, Dilip D. Giri⁴, Stefano Scarpa¹, Manickam Janikariman¹, Narciso Olvera³, Ellen V. Stevens⁵, Qing-Bai She⁵, Carol Aghajanian⁶, Tari A. King³, Elisa de Stanchina⁷, David R. Spriggs⁶, Adriana Heguy⁸, Barry S. Taylor², Chris Sander², Neal Rosen^{5,6}, Douglas A. Levine³, and David B. Solit^{1,6}



ABSTRACT

Effective oncprotein-targeted therapies have not yet been developed for ovarian cancer. To explore the role of phosphatidylinositol 3-kinase (PI3K)/AKT signaling in this disease, we performed a genetic and functional analysis of ovarian cancer cell lines and tumors. PI3K pathway alterations were common in both, but the spectrum of mutational changes differed. Genetic activation of the pathway was necessary, but not sufficient, to confer sensitivity to selective inhibition of AKT and cells with RAS pathway alterations or RB1 loss were resistant to AKT inhibition, whether or not they had coexistent PI3K/AKT pathway activation. Inhibition of AKT1 caused growth arrest in a subset of ovarian cell lines, but not in those with AKT3 expression, which required pan-AKT inhibition. Thus, a subset of ovarian tumors is sensitive to AKT inhibition, but the genetic heterogeneity of the disease suggests that effective treatment with AKT pathway inhibitors will require a detailed molecular analysis of each patient's tumor.

SIGNIFICANCE: A subset of ovarian cancers exhibits AKT pathway activation and is sensitive to selective AKT inhibition. Ovarian tumors exhibit significant genetic heterogeneity and thus an individualized approach based on real-time, detailed genomic and proteomic characterization of individual tumors will be required for the successful application of PI3K/AKT pathway inhibitors in this disease. *Cancer Discovery*; 2(1):56–67. ©2011 AACR.

INTRODUCTION

The phosphatidylinositol 3-kinase (PI3K) pathway is a key regulator of growth factor-mediated proliferation and survival (1). The mechanisms responsible for PI3K/AKT pathway activation in human cancers are diverse and include activating mutations, amplification, or overexpression of *PIK3CA* and *AKT1/2/3*, loss of PTEN expression or function, mutations in the *p85* regulatory subunit of PI3K, RAS mutation, and dysregulation of growth factor receptor and integrin signaling. AKT, which was initially identified as a proto-oncogene in the mouse leukemia virus Akt8 (2), has strong oncogenic function and is a key mediator of PI3K pathway function. AKT isoforms are phosphorylated at high levels in a broad array of human tumor types, including ovarian cancers (3–5). Immunohistochemical studies demonstrate that AKT activation is common in high-grade, late-stage serous ovarian carcinomas (6–9) and may therefore play a role in mediating the progression of these tumors. Furthermore, a multiplatform genomic analysis by The Cancer Genome Atlas (TCGA) Research Network identified alterations in the PI3K/

AKT and RAS pathways in approximately 45% of high-grade, serous ovarian tumors (10).

Here, we performed an integrated analysis of ovarian cancer cell lines and tumors to characterize the mechanisms and functional significance of AKT activation and the potential clinical utility of selective, allosteric AKT inhibitors in patients with this disease. We found that a subset of ovarian cancer cell lines and tumors harbored genetic alterations in the PI3K/AKT pathway. AKT activation was necessary but not sufficient to confer pathway dependence and cells with RB1 loss or RAS or RAF mutation were resistant to AKT inhibition, irrespective of pathway activation. Finally, selective AKT1 inhibition was sufficient for maximal antitumor effects in a subset of ovarian cancer cell lines, whereas pan-AKT inhibition was required in those expressing AKT3. In sum, the results suggest that a detailed genomic and functional analysis of components of the RAS and PI3K/AKT pathways in individual patients with ovarian cancer will be required for effective application of inhibitors of these signaling pathways in this genetically heterogeneous disease.

RESULTS**Functional and Genomic Analysis of Ovarian Cancer Cell Lines Identifies an AKT-Dependent Subset**

AKT pathway activation is common in high-grade, late-stage serous ovarian carcinomas (6–9). We asked whether the growth and survival of ovarian cancer cells with mutational activation of the AKT pathway was dependent on AKT kinase activity by examining the sensitivity of a panel of ovarian cancer cell lines to selective, allosteric inhibitors of AKT as a function of their genotype. We characterized a panel of 17 ovarian cancer cell lines (Supplementary Tables S1 and S2) for mutations and copy number alterations that would be predicted to result in PI3K and/or RAS pathway activation (see Methods). *PIK3CA* mutations (H1047R and E545K), *ERBB2* and *AKT2* amplification, and *PTEN* mutation were identified in 6 of the 17 ovarian cancer cell lines (35%) (Supplementary Table S2 and Supplementary Fig. S1) (11–13). Four of the

Authors' Affiliations: ¹Human Oncology and Pathogenesis Program, the Departments of ²Computational Biology, ³Surgery, ⁴Pathology, ⁵Molecular Pharmacology and Chemistry, and ⁶Medicine, the ⁷Antitumor Assessment Core Facility, and the ⁸Geoffrey Beene Translational Oncology Core Facility, Memorial Sloan-Kettering Cancer Center, New York, New York

S. Scarperi is currently affiliated with the European Gynecology Endoscopy School in Negrar, Verona, Italy. Q-B. She is currently affiliated with the Department of Molecular Pharmacology and Chemistry, University of Kentucky, Lexington, Kentucky.

Note: Supplementary data for this article are available at *Cancer Discovery* Online (<http://www.cancerdiscovery.aacrjournals.org>).

All IHC images can be found at http://cbio.mskcc.org/cancergenomics/hanrahan_2011/.

Corresponding Author: David B. Solit, Memorial Sloan-Kettering Cancer Center, Human Oncology and Pathogenesis Program, 1275 York Avenue, Box 52, New York, NY 10471. Phone: 646-888-2641; Fax: 212-988-0701; E-mail: solitd@mskcc.org

doi: 10.1158/2159-8290.CD-11-0170

©2011 American Association for Cancer Research.

17 ovarian cancer cell lines (23.5%) had RAS/RAF pathway aberrations, including focal KRAS amplification in SKOV-8 (Fig. 1A), KRAS G12V mutation in OVCAR-5, concurrent BRAF V600E and MEK1 mutations in ES2, and a BRAF exon 12 deletion in OV-90 (Supplementary Table S2) (11, 14). In addition, one cell line, SKOV-433, had a focal RB1 deletion (Fig. 1A).

We asked whether the copy number aberrations or mutations identified correlated with levels of protein expression (Fig. 1B). In 2 of the 3 PTEN-mutated cell lines (IGROV-1 and SKOV-6), expression of PTEN protein was not detected; the third (A2780) expressed low levels. Focal deletion of RB1 in SKOV-433 cells was also associated with complete loss of RB1 protein expression. Immunoblot analysis revealed four additional cell lines with no detectable RB1 protein (SKOV-6, CAOV-3, OV-1847, and PEO-4) despite each having copy-neutral aCGH profiles and no somatic mutations within the RB1 gene. High expression levels of AKT2 in OVCAR-3, HER2/neu in SKOV-3, and KRAS in SKOV-8 were consistent with the gene amplification events detected by aCGH. Overall, our integrated genomic and proteomic analyses identified 4 cohorts of ovarian cancer cell lines: those with (i) PI3K pathway alterations; (ii) RAS/RAF pathway aberrations; (iii) RB1 loss; and (iv) wild-type for all the preceding alterations.

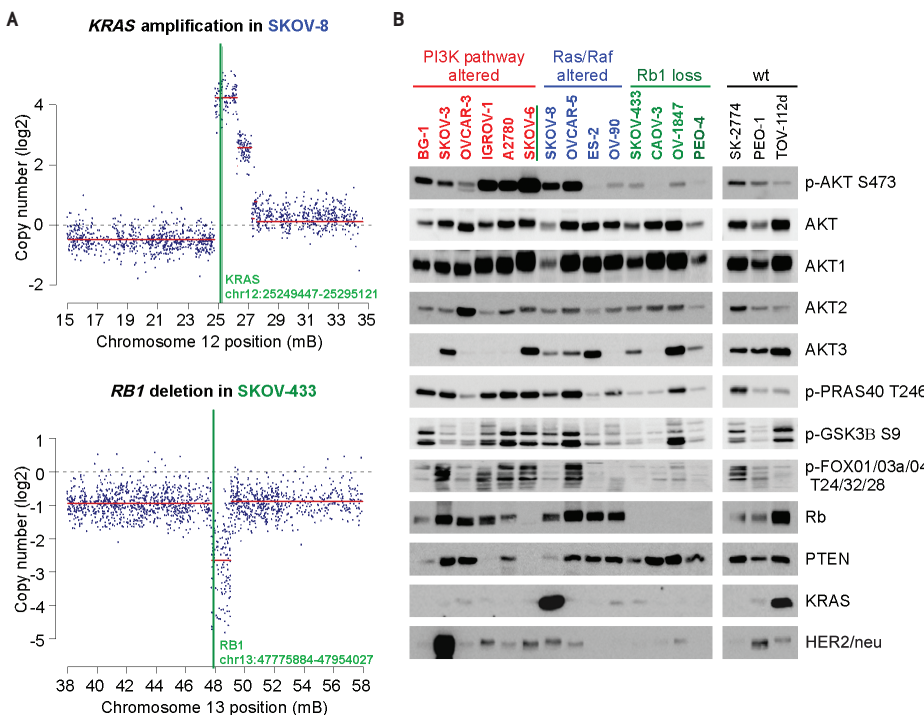
To assess whether alterations in components of the PI3K/AKT pathway resulted in activation of AKT signaling, we evaluated the phosphorylation and abundance of AKT family members and downstream targets (Fig. 1B). Phosphorylation of AKT at serine 473 (p-AKT S473) was used as a surrogate of pathway activity. Elevated levels of p-AKT S473 correlated with the presence of a PI3K pathway or RAS alterations (Fig. 1B), whereas cell lines with BRAF mutation and RB1 loss had low levels. In contrast to this pattern of p-AKT

expression, the levels of AKT substrates such as PRAS40, GSK3 β , and FOXO varied significantly across the panel. Levels of AKT1, AKT2, and AKT3 varied among the cell lines, although AKT3 protein was undetectable in 4 of the 6 cell lines with PI3K pathway alterations.

Selective Inhibition of AKT1/2 Is Sufficient to Inhibit Cell Growth in a Subset of Ovarian Cancer Cell Lines and Xenografts

The dependence of tumor cells on AKT kinases was evaluated by determining their sensitivity to selective pharmacologic inhibitors of the enzymes. We compared two PH-domain-dependent, allosteric inhibitors of AKT that varied in their potency for AKT3 (15–22). The AKT1/2 inhibitor (AKTi1/2) inhibits AKT1 and AKT2 with EC₅₀ values of 3.5 nM and 42.1 nM, respectively, and is significantly less potent against AKT3 with an EC₅₀ of 1.9 μ M in *in vitro* kinase assays (15). The pan-AKT1/2/3 inhibitor (hereafter referred to by its clinical name, MK2206) potently inhibits all three AKT isoforms with EC₅₀ values of 8, 12, and 65 nM for AKT1, AKT2, and AKT3, respectively (16, 17). As depicted in Figure 2A, the IC₅₀ and IC₉₀ values for each cell line were calculated after their exposure to either of these drugs for 5 days (see Methods). The results indicate that the majority of ovarian lines exhibited only a limited response or were completely resistant to AKT inhibition (Fig. 2A, right panel, IC₉₀ \geq 3.0 μ M) despite rapid downregulation of p-AKT expression in sensitive and resistant models by both drugs (Fig. 2B). Mutations in components of the PI3K pathway or in RAS can activate PI3K signaling. Notably, all cell lines that were hypersensitive to both inhibitors (IC₅₀ < 1 μ M) harbored PI3K pathway alterations (SKOV-3, OVCAR-3, IGROV-1, A2780, in red). However, the presence of an AKT pathway alteration was insufficient to confer drug sensitivity

Figure 1. Genomic and proteomic profiling of ovarian cancer cell lines. **A**, probe-level (blue dots) and segmentation data (red lines) from Agilent 244K arrays identifying representative focal amplification (KRAS in SKOV-8) and focal homozygous deletion (RB1 in SKOV-433) events. The vertical green line crosses the x-axis at the chromosomal position of the gene. Y-axis indicates log₂ copy number signal. **B**, immunoblot analysis of the ovarian cancer cell line panel for expression of AKT1/2/3, phosphorylated AKT (Ser473), and activation and abundance of key downstream targets. Cells were arranged based on the presence of PI3K/AKT (red) or RAS/RAF-pathway alterations (blue) and RB1 loss (green and green underline).



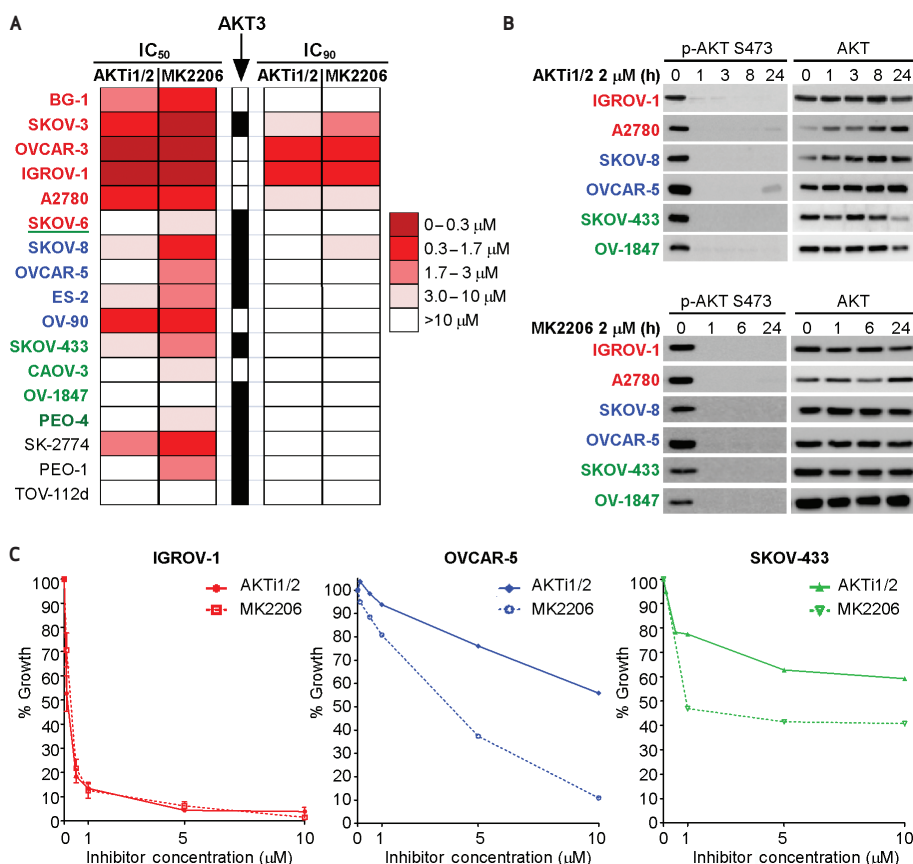


Figure 2. AKT dependence of ovarian cancer cell lines. **A**, IC₅₀ and IC₉₀ values for the AKT1/2 inhibitor (AKT1/2) and panAKT 1/2/3 inhibitor (MK2206) were calculated after treatment with 0 to 10 μM of each inhibitor for 5 days. Drug concentrations are represented by color block gradations from dark red (0–0.3 μM) to bright red (0.3–1.7 μM), dark pink (1.7–3 μM), pale pink (3–10 μM), and white (>10 μM). Cells with detectable AKT3 expression are indicated by black boxes. Cell lines are colored based on the presence of PI3K/AKT (red) or RAS/RAF-pathway (blue) alterations and RB1 loss (green and green underline) as in Figure 1B. **B**, cells were treated for 0 to 24 hours with AKT1/2 or MK2206 (2 μM) and lysates immunoblotted for p-AKT S473 and total AKT. **C**, day 5 dose-response plots of three representative cell lines (IGROV-1, hypersensitive to AKT inhibition, red; OVCAR-5, heightened sensitivity to pan-AKT inhibition, blue; SKOV-433, resistant to AKT inhibition, green).

as exemplified by BG-1 (PIK3CA E545K mutant) and SKOV-6 (PTEN/RB1 null), both of which were resistant to AKT inhibition. Furthermore, tumors with KRAS alterations and high levels of AKT phosphorylation (SKOV8, OVCAR5) were relatively resistant to AKT inhibition. These results suggest that although PI3K is a RAS effector that may be required for RAS-dependent transformation, the maintenance of growth deregulation of such tumors is not AKT dependent.

A subset of cell lines was more sensitive to MK2206 than the AKT1/2 inhibitor (Fig. 2A), suggesting that AKT3 activity may be important in some ovarian tumors and that isoform-selective inhibitors would be ineffective in such models. To further characterize these differences, detailed dose-response curves were generated with cells falling into one of three classes (Fig. 2C). The first class included cell lines with PI3K pathway alterations that expressed AKT1 and AKT2 but not AKT3 (e.g., PTEN-mutant IGROV-1 cells). Such cells were hypersensitive to both MK2206 and AKT1/2. A second cohort of cell lines expressed all three AKT isoforms (e.g., KRAS G12V mutant OVCAR-5 cells), and in such cells, MK2206 was significantly more potent than AKT1/2. Finally, a third cohort represented by the RB1-deleted SKOV-433 cell line was resistant to high concentrations of both AKT inhibitors.

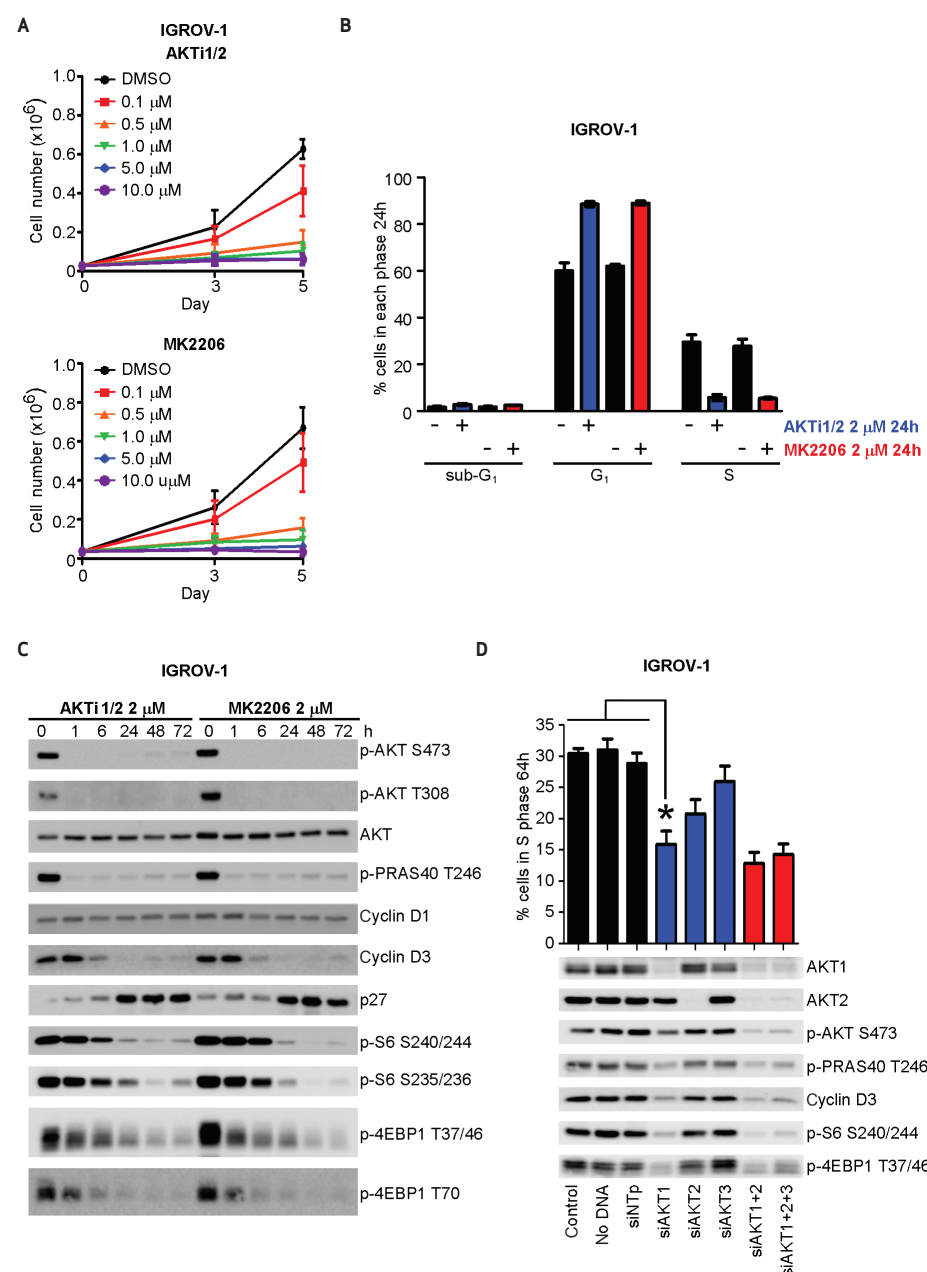
AKT1 Is the Dominant Isoform Driving Cell Proliferation in PTEN-Mutant IGROV-1 Cells

To further define the AKT isoform(s) responsible for AKT dependence in ovarian cancer cells, we investigated the

consequences of pan-AKT and AKT1/2-selective inhibition in PTEN-mutant IGROV-1 cells and xenografts. In this cell line, the effects of both drugs on proliferation were virtually indistinguishable (Figs. 2C and 3A). Fluorescence-activated cell sorting (FACS) analysis confirmed that treatment with either inhibitor caused G₁ growth arrest and loss of cells in the S phase, although no apoptosis was observed (Fig. 3B and data not shown). Immunoblotting demonstrated that both drugs potently inhibited the phosphorylation of AKT on both activation sites (S473 and T308), although the effect on S473 was more durable with MK2206 (Fig. 3C). Both inhibitors also equally downregulated cyclin D3 expression, phosphorylation of PRAS40 (Thr246), a direct target of AKT, and phosphorylation of the downstream translational regulators S6 and 4EBP1 on multiple sites while coordinately increasing p27 expression (Fig. 3C). In summary, inhibition of the AKT1 and AKT2 isoforms using a selective, allosteric inhibitor was sufficient to induce a potent cell cycle arrest in PTEN-mutant IGROV-1 cells. These results were recapitulated *in vivo*, as treatment of mice bearing established IGROV-1 xenografts with either AKT1/2 or MK2206 had similar inhibitory effects on AKT phosphorylation and tumor growth (Supplementary Fig. S2). Taken together, our data suggest that in some ovarian cancers, AKT3 inhibition is dispensable for maximal antitumor activity and isoform-selective inhibitors that spare AKT3 are sufficient to inhibit signaling and proliferation.

To distinguish the roles of the AKT1 and AKT2 isoforms in mediating proliferation, IGROV-1 cells were treated with

Figure 3. Consequence of differential AKT isoform inhibition in PTEN-mutant IGROV-1 cells. **A**, IGROV-1 (PTEN-mutant) cells were treated with 0 to 10 μ M of either AKT1/2 or MK2206 and viable cells counted at days 3 and 5. **B**, cell-cycle distribution was determined by FACS for IGROV-1 cells treated with AKT1-1/2 or MK2206 (2 μ M) for 24 hours. **C**, immunoblots after treatment of IGROV-1 cells with either 2 μ M of AKT1/2 or MK2206 for 0 to 72 hours. Lysates were probed for p-AKT (S473 and T308), p-PRAS40 (T246), and cell-cycle and translation regulators as indicated. **D**, control siRNA (siNTp) or siRNA against individual AKT isoforms, alone or in combination, were transfected into IGROV-1 cells followed by incubation for 64 hours. Cells were collected for FACS analysis (asterisk indicates $P \leq 0.0015$, $n \geq 3$) or subjected to immunoblotting.



siRNA pools directed against AKT1, AKT2, or AKT3 alone or in combination. Transfection of cells with siAKT1 or siAKT2, but not the nontargeting control pool siRNA (siNTp), led to effective ($> 90\%$) downregulation of expression of the respective AKT isoforms (Fig. 3D). We could not detect AKT3 knockdown in these cells, because they do not express detectable levels of AKT3 by immunoblot and thus view siAKT3 transfection in IGROV-1 as a control (Supplementary Fig. S3A). Selective knockdown of AKT1, but not AKT2 or AKT3, was sufficient to induce significant G1 arrest, loss of cells in S phase, and downregulation of cyclin D3 expression and S6- and 4EBP1-phosphorylation (Fig. 3D and Supplementary Fig. S3B). Evidence of synergy was not observed after concomitant knockdown of multiple AKT isoforms nor did

combinatorial knockdown of more than one isoform induce apoptosis (Fig. 3D and Supplementary Fig. S3B). Overall, the effects of AKT1 knockdown were similar to those of the AKT1/2 and pan-AKT inhibitors, suggesting that AKT1 is the major regulator of cell proliferation in IGROV-1 ovarian cancer cells.

Synergistic Effects of MEK and AKT Inhibitors in PI3K- and RAS-Activated Ovarian Cancer Cells

Concurrent activation of the RAS and PI3K pathways occurs in a significant proportion of human cancers (23, 24) and may necessitate combined therapy to fully abrogate their cooperative effects on proliferation and cap-dependent translation (25). Among the four cell lines with RAS/

RAF pathway aberrations in our panel, the *KRAS*-mutant OVCAR-5 and *KRAS*-amplified SKOV-8 cells had high p-AKT expression (Fig. 1B) as well as elevated levels of activated RAS (Fig. 4A). Notably, these cell lines were all insensitive to inhibition of AKT alone (Fig. 2A).

To determine the dependence of the RAS/RAF altered cohort on MAP kinase pathway activation, cells were treated with PD0325901 (hereafter referred to as PD901), a selective, allosteric inhibitor of MEK1/2 (26–29). PD901 potently downregulated ERK phosphorylation in all cell lines examined but only inhibited the proliferation of the RAS/RAF-altered cells ($IC_{50} \leq 13.0$ nM) (Fig. 4B). Despite their dependence on MEK for proliferation, induction of cell death was not observed with PD901 treatment (Fig. 4C, green bar and data not shown).

In tumors with activation of ERK and AKT signaling, inhibition of both has been shown to be required for effective antitumor activity (25). Neither PD901 nor 2 μ M of MK2206 induced apoptosis in OVCAR-5 cells at 72 hours (Fig. 4C). Treatment with higher concentrations of MK2206 resulted in a marginal increase in cell death, which was significantly enhanced by concurrent MEK inhibition (Fig. 4C, asterisk). Moreover, cotreatment of PD901 and MK2206 synergistically reduced the phosphorylation of p70S6K, S6, and 4EBP1 and decreased

cyclin D3 expression (Fig. 4D). Cotreatment with the pan-caspase inhibitor ZVAD-FMK or QVD-OPH abrogated the increase in cell death observed with combination treatment, confirming that this effect was the result of synergistic induction of apoptosis (Supplementary Fig. S4A). A similar induction of apoptosis and inhibition of downstream signaling was also observed in OVCAR-5 cells after concomitant knockdown of KRAS expression by siRNA and treatment with MK2206 at 10 μ M (Supplementary Fig. S4B). Finally, consistent with the *in vitro* results, enhanced antitumor activity was observed with the combination of PD901 and MK2206 in mice bearing established *KRAS*-mutant OVCAR-5 xenografts (Supplementary Fig. S4C).

Induction of cell death was significantly greater in OVCAR-5 cells when PD901 was combined with the pan-AKT inhibitor MK2206 as compared with the isoform-selective inhibitor AKT1/2 (Fig. 4C). To further define the role of AKT3 in promoting cell survival in this context, we stably infected OVCAR-5 cells with lentiviral shRNAs targeting AKT3 or a scrambled control. Concurrent treatment with PD901 and AKT1/2 resulted in induction of cell death only in OVCAR-5 cells with stable expression of AKT3 shRNAs but not in cells infected with a scrambled control hairpin (Supplementary Fig. S5). These results suggest that AKT3 may function redundantly with AKT1 and AKT2 to promote the survival of a subset of ovarian cancers.

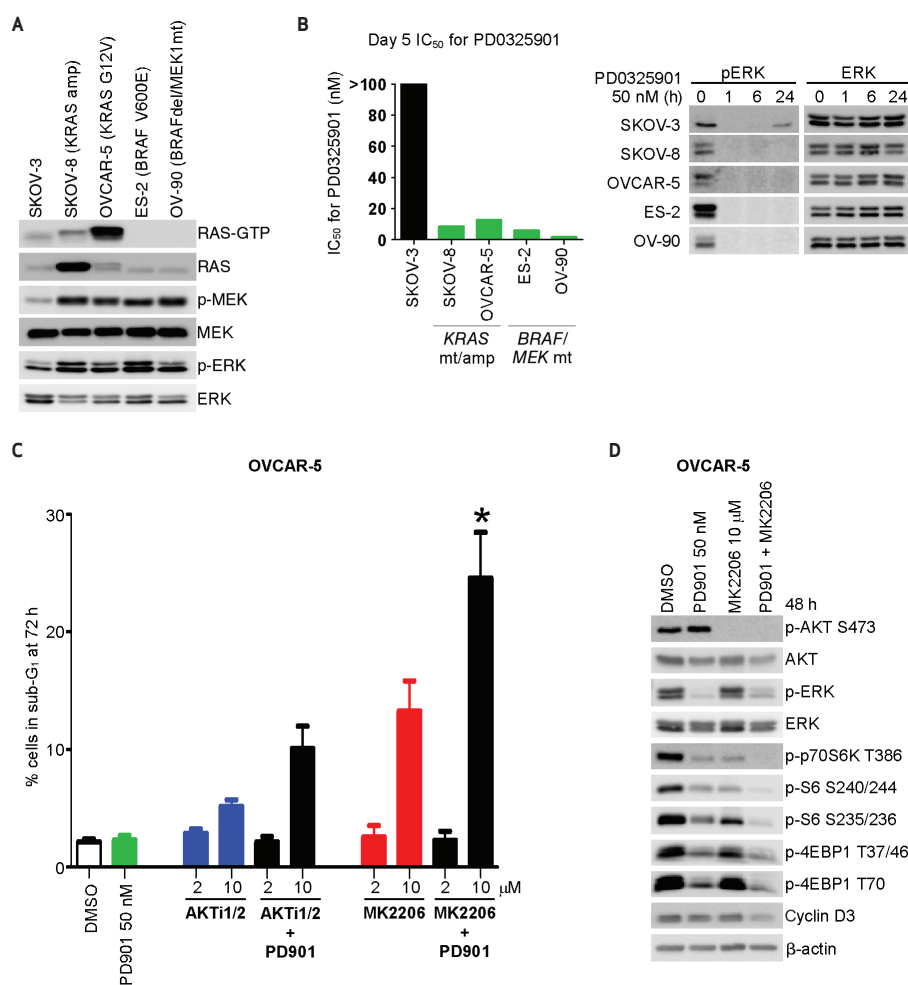
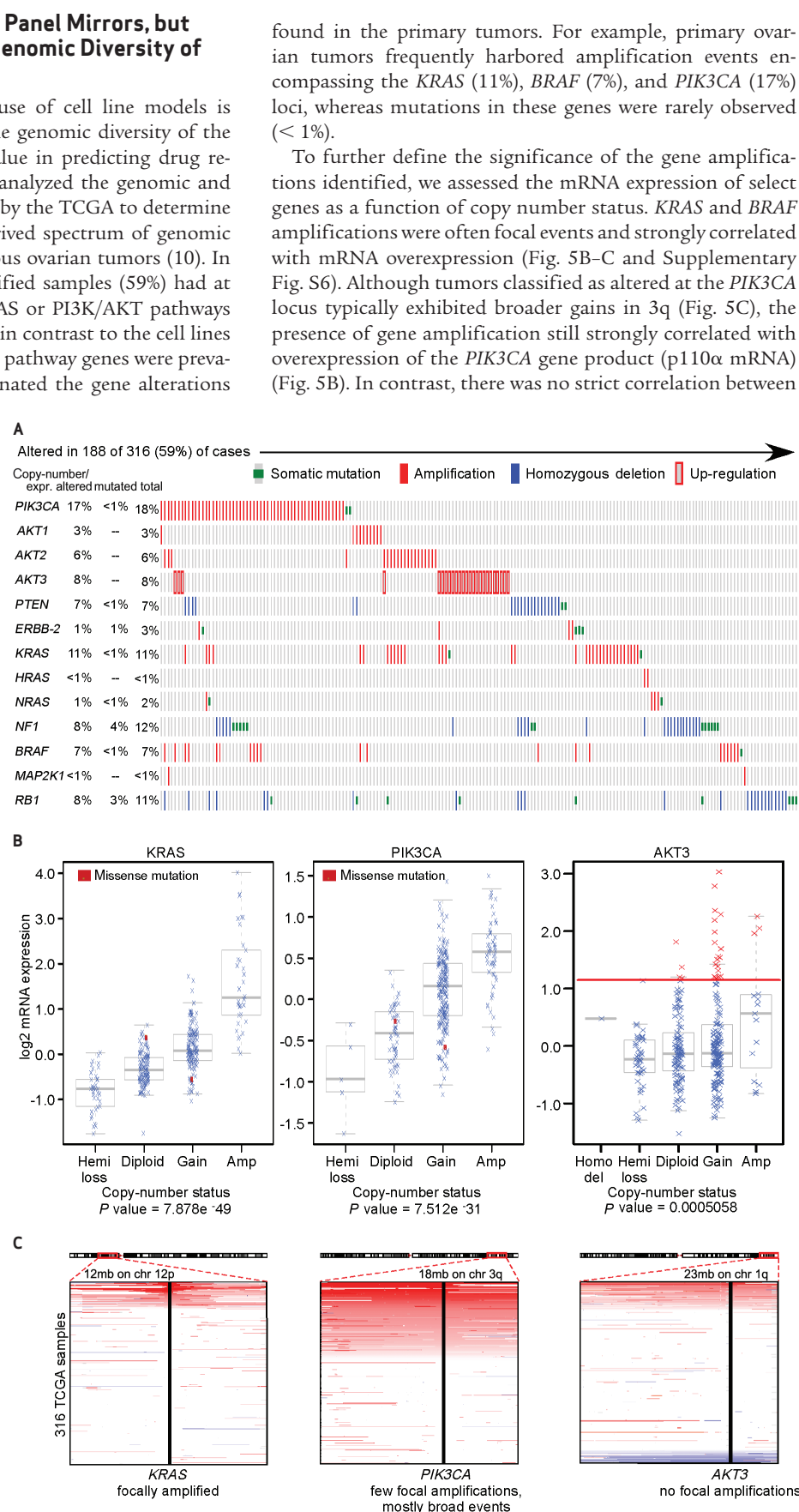


Figure 4. RAS/RAF pathway-activated ovarian cancer cells exhibit MEK dependence and synergistic induction of apoptosis with combined MEK/AKT inhibition. **A**, levels of activated RAS (RAS-GTP) were determined by pulldown of GTP-bound RAS using recombinant RAS binding domain of RAF. Input lysates were also immunoblotted as shown. **B**, IC_{50} values for the allosteric inhibitor of MEK1/2, PD0325901 (PD901) were calculated after treatment with 0 to 500 nM of inhibitor for 5 days. Immunoblots for p-ERK and ERK after treatment with PD901 (50 nM) for 0 to 24 hours. **C**, induction of cell death after combined treatment with 50 nM PD901 and increasing doses of either AKT1/2 or MK2206 (2 or 10 μ M) was measured by FACS analysis at 72 hours in OVCAR-5 cells. Maximal cell death was induced after cotreatment with PD901 and MK2206 (asterisk indicates $P \leq 0.0287$ versus all other treatments, $n \geq 3$). **D**, OVCAR-5 cells were treated with PD901 (50 nM) or MK2206 (10 μ M) alone or in combination for 48 hours and lysates were immunoblotted.

The Ovarian Cancer Cell Line Panel Mirrors, but Does Not Fully Reflect, the Genomic Diversity of Ovarian Tumors

One major limitation of the use of cell line models is that they may not recapitulate the genomic diversity of the human disease and thus their value in predicting drug response may be limited. We thus analyzed the genomic and mRNA expression data generated by the TCGA to determine the prevalence of the cell line-derived spectrum of genomic alterations in 316 high-grade serous ovarian tumors (10). In total, 188 of the 316 TCGA-qualified samples (59%) had at least one alteration within the RAS or PI3K/AKT pathways or within *RB1* (Fig. 5A). However, in contrast to the cell lines in which point mutations in these pathway genes were prevalent, copy number changes dominated the gene alterations

Figure 5. The ovarian cancer cell lines modestly recapitulate the spectrum of mutations found in primary ovarian tumors. **A**, heat map showing the concordance of PI3K and RAS pathway alterations and *RB1* deletions/mutations for 316 serous ovarian cancer TCGA samples. Amplifications are indicated in solid red, homozygous deletions in solid blue, and somatic mutations in green. Overexpression of AKT3 is indicated by a hollow, red rectangle. **B**, log₂ mRNA expression was assessed as a function of GISTIC-based DNA copy number calls (homozygous deletion, hemizygous loss, diploid, gain, high-level amplification) across all samples. *P* values were generated using analysis of variances. The red line in the AKT3 box plot indicates the cutoff for samples with significant mRNA overexpression (red "x") as defined by > 2 standard deviations of the mean of the samples that are diploid/copy-neutral for AKT3. **C**, copy number heat maps demonstrating the focality of the amplifications encompassing the KRAS, PIK3CA, and AKT3 loci. X-axis illustrates the copy number status (red: amplification, white: copy neutral, blue: deletion) of the indicated gene for each of the 316 TCGA samples listed on y-axis.



found in the primary tumors. For example, primary ovarian tumors frequently harbored amplification events encompassing the *KRAS* (11%), *BRAF* (7%), and *PIK3CA* (17%) loci, whereas mutations in these genes were rarely observed (< 1%).

To further define the significance of the gene amplifications identified, we assessed the mRNA expression of select genes as a function of copy number status. *KRAS* and *BRAF* amplifications were often focal events and strongly correlated with mRNA overexpression (Fig. 5B–C and Supplementary Fig. S6). Although tumors classified as altered at the *PIK3CA* locus typically exhibited broader gains in 3q (Fig. 5C), the presence of gene amplification still strongly correlated with overexpression of the *PIK3CA* gene product (p110 α mRNA) (Fig. 5B). In contrast, there was no strict correlation between

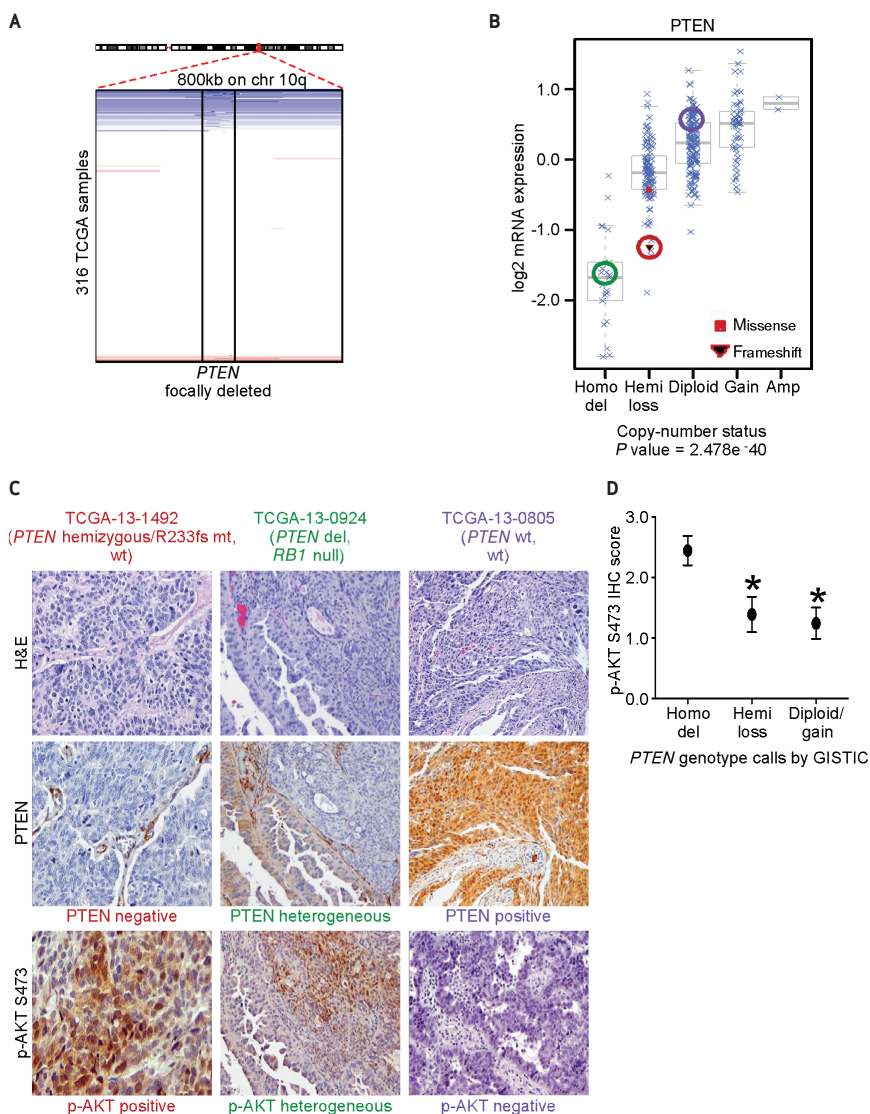


Figure 6. PTEN genotype frequently dictates PTEN expression status, but evidence of heterogeneous staining implies polyclonality within some ovarian tumors. **A**, copy number heat map of the ovarian TCGA samples showing that a subset harbor focal deletion of the *PTEN* locus. X-axis represents the copy number status (blue: deletion, white: copy neutral, red: amplification) of the *PTEN* gene for each of the 316 TCGA samples listed on y-axis. **B**, log₂ mRNA expression as a function of GISTIC-based copy number status at the *PTEN* locus (*P* values as indicated, analysis of variance). Circled tumors indicate PTEN mRNA and copy number status of the corresponding tumors in part C. **C**, hematoxylin and eosin (H&E), PTEN, and p-AKT S473 immunohistochemistry of representative ovarian TCGA tumors with PTEN-negative, heterogeneous, and positive staining. **D**, mean p-AKT S473 IHC scores as a function of GISTIC-based copy number calls at the *PTEN* locus. Dots represent average p-AKT IHC score \pm SE for each group (asterisks indicate $P \leq 0.0276$ versus PTEN homozygous deleted).

AKT3 mRNA overexpression and the degree of amplification nor were there any focal *AKT3* amplification events (Fig. 5B–C). Elevated AKT3 mRNA expression, however, was observed in 8% of tumors, including those characterized as diploid at the *AKT3* locus (Fig. 5A–B). This suggests that gene amplification is not the primary determinant of AKT3 expression in serous ovarian cancers. This does not hold true for *AKT2*, for which focal amplification was common (6%) and strongly correlated with mRNA overexpression (Fig. 5A and Supplementary Fig. S6). Thus, whereas *AKT2* overexpression is secondary to a genetic event in some ovarian cancers, the etiology of AKT3 overexpression is unknown and may be the result of yet to be elucidated epigenetic factors.

Among the deletion events found in the TCGA data set, homozygous loss of *PTEN* (7%), *RB1* (8%), and *NFI* (8%) were common (Fig. 5A). These deletions were typically focal and were strongly associated with loss of mRNA expression in all three instances (Fig. 6A–B and Supplementary Fig. S7). To gain insight into the functional relevance of these events, we assessed *PTEN* expression and AKT activation by immunohistochemistry (IHC) in 52 of the 316

TCGA tumors and correlated these results with GISTIC-based genotype calls and mRNA expression. In 8 of 52 (15.4%) tumors, *PTEN* protein expression was absent in all areas of the tumor (Fig. 6C and Supplementary Table S3, Supplementary Fig. S8, and http://cbio.mskcc.org/cancergenomics/hanrahan_2011/). All eight of these cases demonstrated *PTEN* copy number loss with five scored as homozygous deleted by GISTIC and three as hemizygous loss at the *PTEN* locus. Of the latter three, one sample (TCGA-13-1492) harbored a frameshift mutation (R233fs*22) in *PTEN*. Six of the eight tumors had correspondingly reduced log₂ mRNA values less than -1.2 (with no mRNA data available on one tumor). Consistent with the IHC data, *PTEN* homozygous deletion was also associated with low protein levels by reverse-phase proteomic array (RPPA) analysis (Supplementary Fig. S9A). High levels of AKT phosphorylation by IHC (Fig. 6C–D) and by RPPA analysis (Supplementary Fig. S9B) also correlated with *PTEN* homozygous deletion. In contrast, significantly lower levels of AKT phosphorylation were found in the *PTEN*-hemizygous loss and *PTEN*-diploid/gain cohorts with no difference found between these latter two groups (Fig. 6C–D).

Thirty-six of 52 (69.2%) tumors stained uniformly positive for PTEN expression (Fig. 6C and Supplementary Table S3). Sixteen were scored as *PTEN* copy number neutral (diploid), 8 as copy number gain, and 11 demonstrated hemizygous loss at the *PTEN* locus, all with virtually neutral mRNA expression levels. One *PTEN*-positive tumor (TCGA-13-1405) was scored as homozygous-deleted for *PTEN* based on the GISTIC analysis. A second scoring method (RAE), however, characterized this sample as single copy loss at the *PTEN* locus (Supplementary Table S3, in red). These results highlight the challenges of computationally predicting the functional relevance of genomic alterations from array data of tumors with complex karyotypes and mixed cell populations.

Finally, 8 of 52 (15.4%) tumor samples had a heterogeneous pattern of *PTEN* loss and corresponding p-AKT S473 overexpression (Fig. 6C and Supplementary Table S3). Both the RAE and GISTIC analyses characterized three of these heterogeneously staining tumors as *PTEN*-homozygous deleted. Because the *PTEN*-positive component of each of these tumors comprised less than 20% of the overall tumor content, these results are consistent with the existence of a polyclonal population of tumor cells, the majority of which have homozygous *PTEN* deletions and corresponding loss of *PTEN* expression.

DISCUSSION

Ovarian cancer is a histologically and genetically complex disease (4, 30–32). Morphologically, ovarian cancers can be divided into type I low-grade, low-malignant potential tumors and type II high-grade, serous carcinomas, carcinosarcomas, and undifferentiated carcinomas. Although outcome has improved recently for patients in the latter group, with 5-year survival rates now approaching 50%, the cure rate remains low at approximately 30% (33–35). Genomic characterization of type II tumors suggests that alterations in the *TP53* and/or *BRCA1/2* genes occur early in their pathogenesis and cooperate to promote genomic instability. This genomic instability results in diverse subsequent events that are believed to drive ovarian tumor growth and metastatic progression, including alterations that activate the PI3K/AKT pathway (3–5, 36).

Because phosphorylated AKT is expressed at high levels in the majority of high-grade, serous ovarian cancers, we sought to define the AKT dependence of ovarian cancer cell lines with the goal of identifying genomic signatures predictive of drug sensitivity. Using an integrative approach, we were able to define four classes of ovarian cancer cells: cells with (i) PI3K/AKT pathway alterations; (ii) RAS/RAF/MEK1 alterations; (iii) RB1 loss; and (iv) those wild-type for all the preceding pathways and genes. Although PI3K/AKT pathway activation was common and correlated with AKT dependence, pathway activation was the result of diverse underlying molecular events and pathway activation alone was not sufficient to confer AKT inhibitor sensitivity. Notably, all cell lines with RAS/RAF alterations and those with RB1 loss, including those expressing high levels of phosphorylated AKT, exhibited intermediate or high levels of resistance to AKT inhibition. These results support the testing of AKT pathway inhibitors in patients with serous ovarian cancer but suggest that AKT inhibition alone will be effective in only a subset of patients.

Given the central role of AKT signaling in normal cellular physiology, there is particular concern that inhibitors of this pathway may exhibit a narrow therapeutic index. One potential approach to minimizing toxicity when targeting this pathway is to selectively inhibit only those AKT isoforms within a specific tumor that promote transformation and/or progression. Each of the three AKT isoforms has been implicated as playing a dominant role in select cancer types (8, 37–42). Our analysis of the ovarian cancer cell line panel revealed that AKT1 and AKT2 were ubiquitously expressed, whereas AKT3 expression was detectable in only a subset of cell lines. Moreover, only a subset of the TCGA tumors expressed a high level of AKT3 mRNA. Based on these data, we hypothesized that AKT3 inhibition may not be required in some ovarian tumors for maximal antitumor effect. To address this question, we used two highly selective, allosteric inhibitors of AKT that differed only in their potency for AKT3. In AKT3-deficient models such as the *PTEN*-mutant IGROV-1 cell line, the effects of the pan- and AKT1/2-selective inhibitors were identical. Furthermore, knockdown studies using isoform-selective siRNA suggested that AKT1 was the dominant AKT isoform driving proliferation in these cells and that AKT3 inhibition was dispensable. In contrast, a subset of cells expressing AKT3 was sensitive to the pan-AKT inhibitor MK2206 but resistant to the AKT1/2. In sum, the data suggest that an AKT isoform-selective approach may be of use in a subset of patients but that pan-AKT inhibition will be required in others.

One limitation of cell lines is that they may not accurately reflect the genomic profile of the cancer lineage that they purport to model and thus may not be predictive of clinical efficacy. Such cell line bias may arise because some genetic lesions (e.g., *KRAS/BRAF* mutation) may provide a selective advantage to growth in culture (43). Through serial passage, cell lines may also drift or acquire additional genetic changes that were not present in the initial tumor. To address these issues, we compared the genomic profile of our ovarian cancer cell line panel with that of 316 high-grade, serous ovarian cancers within the TCGA data set (10). Our analysis indicated that although PI3K/AKT, RAS/RAF, and RB1 alterations were common in both the cell line and tumor panels, the specific molecular alterations present within the tumors were only loosely recapitulated within the cell lines. For example, although *PIK3CA* amplification was common (17%) and *PIK3CA* mutations were rare (1%) in serous ovarian tumors, consistent with other ovarian cancer cell line studies, *PIK3CA* mutations were overrepresented within the cell line panel, whereas not a single ovarian cancer cell line harbored focal *PIK3CA* amplification (13). Similarly, *KRAS* amplification was common in the tumors (11%) but only present in a single cell line, SKOV-8. SKOV-8 cells did express high levels of RAS-GTP and were MEK-dependent, and their response to MEK and AKT inhibitors was similar to those of the OVCAR-5 cell line, which expresses a *KRAS* G12V allele, a mutation found in less than 1% of serous ovarian cancers. Differences between *KRAS* amplification and mutation, however, may become apparent with further study and thus it would be inappropriate to consider OVCAR-5 as a representative model for the larger cohort of RAS-altered ovarian tumors, most of which exhibit amplification of wild-type *KRAS*. In summary, the data suggest that the currently available ovarian cancer cell lines only

modestly reflect the genomic complexity of the human disease and that a richer panel of ovarian cancer cell lines with multiple representative examples derived from each genetic class is needed.

Our integrated analysis of the cell line and tumor panels also highlights the difficulty of using array-based copy number data to identify those patients with functional gene amplifications and deletions. In the case of *PTEN*, copy number status as scored by either the GISTIC or RAE algorithms correlated strongly with *PTEN* mRNA expression. Further, *PTEN* copy number-neutral (diploid) or homozygous deletion calls were good predictors of the presence or loss of *PTEN* protein and levels of p-AKT expression by IHC and RPPA analysis. However, hemizygous loss of the *PTEN* gene did not reliably correlate with functional loss of *PTEN* protein expression by IHC or downregulation of *PTEN* mRNA expression. These results suggest that in the absence of homozygous deletion, copy number data alone were inadequate to accurately characterize *PTEN* status. A heterogeneous pattern of *PTEN* expression by IHC was also common, suggesting that clonal heterogeneity will prove to be an additional hurdle to the use of array-based platforms to accurately identify tumors with functional loss of *PTEN*.

In summary, our data suggest that the activity of AKT inhibitors will be restricted to tumors harboring genomic alterations within the pathway and that combination therapy will be required to elicit a tumor response or regression in most tumors. On the basis of these data, we predict a low response rate with selective AKT pathway inhibitors when such agents are used alone in ovarian cancers. This reality may necessitate the development of such compounds initially in cohorts of patients from other tumor lineages in which the frequency of defined PI3K/AKT pathway alterations is high. Agents shown to potently inhibit pathway activity in such tumors with an acceptable therapeutic index could then be tested in a combinatorial fashion in ovarian cancer using a truly individualized approach based on real-time, detailed genomic and proteomic characterization of individual tumors.

METHODS

Cell Lines and Culture Conditions

AKT1/2 inhibitor (AKTi1/2, compound 17) (15) and pan-*AKT*1/2/3 inhibitor (MK2206) (16, 17) were obtained from Merck. PD0325901 (PD901) was synthesized as reported (26–29). ZVAD-FMK and QVD-OPH were from BD Pharmingen and R&D Systems, respectively. The human ovarian cancer cell lines SKOV-3/SKOV-8/CAOV-3 (DME), OVCAR-3/A2780 (RPMI 1640), and OV-1847/PEO-4 (M5) were provided by David Spriggs (MSKCC) and BG-1/SKOV-6/OVCAR-5/SKOV-433/PEO-1 (M5) and IGROV-1/SK-2774 (RPMI 1640) by Douglas A. Levine (MSKCC), and are available on request. ES-2 (McCoy's) and OV-90/TOV-112d (MCDB105:199 Earle's) were purchased from American Type Culture Collection. Cells were maintained at 37°C in 5% CO₂ in media indicated in parentheses, supplemented with 2 mM glutamine, 50 units/mL each of penicillin and streptomycin, and 10% fetal bovine serum (PAA Laboratories).

Genomic Studies

Genomic DNA was extracted using the DNAeasy Tissue Kit (Qiagen). Mutations in *NRAS*, *KRAS*, *MEK1*, *BRAF*, *PIK3CA*, and *AKT1* were screened by Sequenom MassARRAY assay (43). As

previously described, all detected mutations were confirmed by conventional Sanger sequencing of coding exons (44). Additionally, all coding exons of *AKT2*, *AKT3*, *RB1*, and *PTEN* were screened for mutations by Sanger biochemistry. Primer sequences used for exon amplification are available on request.

Array Comparative Genomic Hybridization

Labeled DNA was cohybridized to Agilent 244K CGH microarrays with a pool of female reference normal DNA. Raw copy number data were normalized and segmented as described (45, 46) and were viewed using Agilent Genomic Workbench Standard Edition (5.0.14) software and the publically accessible Broad Institute Integrative Genomics Viewer (IGV) standardized to build 36.1 (hg18) of the reference human genome.

Western Blotting

For Figure 1B, log phase ovarian cancer cell lines were harvested at 70% confluence subsequent to an 18-hour refreshment of media. For time courses, cells were treated for the indicated doses and times. Cells were lysed in 1% NP-40 lysis buffer and processed for immunoblotting as described (44). Anti-cyclin D1, cyclin D3, KRAS, and *PTEN* antibodies were from Santa Cruz Biotechnology. Anti-p27 was from BD Transduction Labs. Anti-ERBB2 was from Neomarkers. Anti-pPRAS40-T246 and AKT3 were from Millipore. All other antibodies were from Cell Signaling Technology. Proteins were visualized using the Fuji LAS-4000 (GE Lifesciences). Each immunoblot shown is representative of $n \geq 3$.

Proliferation Assays/Fluorescence Activated Cell Sorting Analysis

Cells were plated and the next day either harvested for counting (day 0) or treated with serial dilutions of drug (0–10 μM for AKTi1/2 and MK2206; 0–500 nM for PD0325901) or DMSO control. Cells were incubated for 3 to 5 days and counted using the Vi-CELL XR 2.03 (Beckman Coulter). From the averages of at least two experiments in duplicate (\pm SE), IC₅₀ curves were generated by plotting percent growth [(mean cell number at drug dose D5 – mean cell number of control D0)/(mean cell number of DMSO D5 – mean cell number of control D0) × 100] against drug concentration. IC_{50/90} values were calculated using Graphpad Prism 5. For FACS, floating and adherent cells were collected and stained with ethidium bromide as reported (47). FACS graph bars represent mean of $n \geq 3$ (\pm SE). Significant P values < 0.05 were determined by unpaired, two-tailed Student *t* tests.

siRNA Transfections

Cell lines were plated in media without penicillin/streptomycin and transfected with 20 nM of siRNA pools (all from Dharmacon) against human AKT1 (L-003000), AKT2 (L-003001), AKT3 (L-003002), KRAS (L-005069-00), or a nontargeting control pool (D-001810-10) in OPTIMEM (Gibco) with Dharmafect Transfection Reagent #1 (T-2001-03) or reagents alone (no DNA). After 24 hours, transfection media was refreshed. Cells were collected 64 hours after transfection and subject to FACS and immunoblotting as previously with $n \geq 3$.

RAS-GTP Assay

Cells were synchronously plated and harvested at 75% confluence subsequent to an 18-hour refreshment of media according to the Millipore RAS Activation Assay. Briefly, 500 μg of lysate was immunoprecipitated using beads containing the recombinant RAS binding domain of RAF. Beads were washed, boiled with sample buffer, resolved on sodium dodecyl sulphate–polyacrylamide gels, and membranes were probed with pan-RAS antibody to detect levels of GTP-bound, active RAS. Input lysates were also probed for total levels of RAS and indicated proteins. Immunoblots shown are representative of $n = 3$.

Patient Data Collection and Analysis

Genomic analyses were performed on 316 human, high-grade, serous, ovarian cancer samples as part of the TCGA project on ovarian cancer (10). DNA copy number calls were derived from CBSA-segmented Agilent 1 M microarray data and analyzed by GISTIC and RAE algorithms using the R statistical framework (48). mRNA expression was measured using three different platforms (Agilent 244K Whole Genome Expression Array, Affymetrix HT-HG-U133A, and Affymetrix Exon 1.0 arrays), and gene expression values were derived as reported (46). RPPA data were generated on 29 of 316, as previously described (49). For all gene expression analyses, a single log₂ median-centered gene expression data set was created. mRNA expression values were then correlated with the corresponding DNA copy number categories (homozygous deletion, hemizygous loss, diploid, gain, high-level amplification) across all samples as previously described (48). IHC for PTEN was performed as described (50) and scored as negative, heterogeneous, or positive staining. IHC for p-AKT-S473 was performed using an overnight incubation with the primary antibody p-AKT^{T473} (Cell Signaling, clone D9E, 1:40) at +4°C and immunodetection with an avidin biotin-peroxidase complex (Vectastain; Vector). Staining was scored as negative = 0, weak = 1, moderate = 2, or strong = 3. All sections were counterstained with hematoxylin and scored by one technician and one pathologist blinded to genomic information. All IHC images can be found at http://cbio/mskcc.org/cancergenomics/hanrahan_2011/.

Disclosure of Potential Conflicts of Interest

No potential conflicts of interest were disclosed.

Acknowledgments

We thank Juan Qiu and WaiLin Wong for their technical assistance with the *in vivo* drug studies.

Grant Support

This work was funded by the SU2C-AACR-DT0209 Dream Team Translational Research Grant (L. Cantley, C. Sawyers), Ovarian Cancer Research Foundation OCRF PPD Grant (C. Aghajanian), National Institutes of Health grant RO1-CA127240 (D.B. Solit), Mr. William H. Goodwin and Mrs. Alice Goodwin and the Commonwealth Foundation for Cancer Research and The Experimental Therapeutics Center of MSKCC (D.B. Solit), National Cancer Institute grant 1U24CA143840 (C. Sander, M. Ladanyi), David H. Koch Fellowship at MSKCC (B.S. Taylor), Entertainment Industry Foundation Revlon Run/Walk for Women (D.A. Levine), and Department of Defense grant OCRRP W81XWH-10-1-0222 (D.A. Levine).

Received July 12, 2011; revised October 17, 2011; accepted October 28, 2011; published OnlineFirst November 3, 2011.

REFERENCES

- Vanhaesebroeck B, Guillermet-Guibert J, Graupera M, Bilanges B. The emerging mechanisms of isoform-specific PI3K signalling. *Nat Rev Mol Cell Biol* 2010;11:329–41.
- Staal SP. Molecular cloning of the akt oncogene and its human homologues AKT1 and AKT2: amplification of AKT1 in a primary human gastric adenocarcinoma. *Proc Natl Acad Sci U S A* 1987;84:5034–7.
- Bast RC Jr, Hennessy B, Mills GB. The biology of ovarian cancer: new opportunities for translation. *Nat Rev Cancer* 2009;9:415–28.
- Levanon K, Crum C, Drapkin R. New insights into the pathogenesis of serous ovarian cancer and its clinical impact. *J Clin Oncol* 2008;26:5284–93.
- Landen CN Jr, Birrer MJ, Sood AK. Early events in the pathogenesis of epithelial ovarian cancer. *J Clin Oncol* 2008;26:995–1005.
- Yuan ZQ, Sun M, Feldman RI, Wang G, Ma X, Jiang C, et al. Frequent activation of AKT2 and induction of apoptosis by inhibition of phosphoinositide-3-OH kinase/Akt pathway in human ovarian cancer. *Oncogene* 2000;19:2324–30.
- Altomare DA, Wang HQ, Skelton KL, De Rienzo A, Klein-Szanto AJ, Godwin AK, et al. AKT and mTOR phosphorylation is frequently detected in ovarian cancer and can be targeted to disrupt ovarian tumor cell growth. *Oncogene* 2004;23:5853–7.
- Cristiano BE, Chan JC, Hannan KM, Lundie NA, Marmy-Conus NJ, Campbell IG, et al. A specific role for AKT3 in the genesis of ovarian cancer through modulation of G(2)-M phase transition. *Cancer Res* 2006;66:11718–25.
- Kurose K, Zhou XP, Araki T, Cannistra SA, Maher ER, Eng C. Frequent loss of PTEN expression is linked to elevated phosphorylated Akt levels, but not associated with p27 and cyclin D1 expression, in primary epithelial ovarian carcinomas. *Am J Pathol* 2001;158:2097–106.
- Cancer Genome Atlas Research Network. Integrated genomic analyses of ovarian carcinoma. *Nature* 2011;474:609–15.
- Ikediobi ON, Davies H, Bignell G, Edkins S, Stevens C, O'Meara S, et al. Mutation analysis of 24 known cancer genes in the NCI-60 cell line set. *Mol Cancer Ther* 2006;5:2606–12.
- Hung MC, Zhang X, Yan DH, Zhang HZ, He GP, Zhang TQ, et al. Aberrant expression of the c-erbB-2/neu protooncogene in ovarian cancer. *Cancer Lett* 1992;61:95–103.
- Cheung HW, Cowley GS, Weir BA, Boehm JS, Rusin S, Scott JA, et al. Systematic investigation of genetic vulnerabilities across cancer cell lines reveals lineage-specific dependencies in ovarian cancer. *Proc Natl Acad Sci U S A* 2011;108:12372–7.
- Estep AL, Palmer C, McCormick F, Rauen KA. Mutation analysis of BRAF, MEK1 and MEK2 in 15 ovarian cancer cell lines: implications for therapy. *PLoS One* 2007;2:e1279.
- Bilodeau MT, Balitz AE, Hoffman JM, Manley PJ, Barnett SF, Defeo-Jones D, et al. Allosteric inhibitors of Akt1 and Akt2: a naphthyridinone with efficacy in an A2780 tumor xenograft model. *Bioorg Med Chem Lett* 2008;18:3178–82.
- Tolcher AW, Yap TA, Fearon I, Taylor A, Carpenter C, Brunetto AT, et al. A phase I study of MK-2206, an oral potent allosteric Akt inhibitor (Akti), in patients (pts) with advanced solid tumor (ST). *J Clin Oncol*, 2009 ASCO Annual Meeting Proceedings (Post-Meeting Edition) 2009;27:3503.
- Yap TA, Papadopoulos K, Fearon I, Carpenter C, Delgado L, Taylor A, et al. First dose-finding study in cancer patients (pts) of a potent, selective, allosteric AKT inhibitor MK2206 (MK), incorporating pharmacodynamic (PD) and predictive biomarkers and showing profound pathway blockade. *AACR 101st Annual Meeting* 2010;Abstract 27.
- She QB, Chandarlapaty S, Ye Q, Lobo J, Haskell KM, Leander KR, et al. Breast tumor cells with PI3K mutation or HER2 amplification are selectively addicted to Akt signaling. *PLoS One* 2008;3:e3065.
- Chandarlapaty S, Sawai A, Scaltriti M, Rodrik-Outmezguine V, Grbovic-Huezo O, Serra V, et al. AKT inhibition relieves feedback suppression of receptor tyrosine kinase expression and activity. *Cancer Cell* 2011;19:58–71.
- Meng J, Dai B, Fang B, Bekele BN, Bornmann WG, Sun D, et al. Combination treatment with MEK and AKT inhibitors is more effective than each drug alone in human non-small cell lung cancer *in vitro* and *in vivo*. *PLoS One* 2010;5:e14124.
- Liu R, Liu D, Trink E, Bojdani E, Ning G, Xing M. The Akt-specific inhibitor MK2206 selectively inhibits thyroid cancer cells harboring mutations that can activate the PI3K/Akt pathway. *J Clin Endocrinol Metab* 2011;96:E577–85.
- Balasis ME, Forinash KD, Chen YA, Fulp WJ, Coppola D, Hamilton AD, et al. Combination of farnesyltransferase and Akt inhibitors is synergistic in breast cancer cells and causes significant breast tumor regression in ErbB2 transgenic mice. *Clin Cancer Res* 2011;17:2852–62.
- McCubrey JA, Steelman LS, Chappell WH, Abrams SL, Wong EW, Chang F, et al. Roles of the Raf/MEK/ERK pathway in cell growth, malignant transformation and drug resistance. *Biochim Biophys Acta* 2007;1773:1263–84.
- Shaw RJ, Cantley LC. Ras, PI(3)K and mTOR signalling controls tumour cell growth. *Nature* 2006;441:424–30.

25. She QB, Halilovic E, Ye Q, Zhen W, Shirasawa S, Sasazuki T, et al. 4E-BP1 is a key effector of the oncogenic activation of the AKT and ERK signaling pathways that integrates their function in tumors. *Cancer Cell* 2010;18:39–51.
26. Ohren JF, Chen H, Pavlovsky A, Whitehead C, Zhang E, Kuffa P, et al. Structures of human MAP kinase kinase 1 (MEK1) and MEK2 describe novel noncompetitive kinase inhibition. *Nat Struct Mol Biol* 2004;11:1192–7.
27. Sebolt-Leopold JS, Herrera R. Targeting the mitogen-activated protein kinase cascade to treat cancer. *Nat Rev Cancer* 2004;4:937–47.
28. Sebolt-Leopold JS, English JM. Mechanisms of drug inhibition of signalling molecules. *Nature* 2006;441:457–62.
29. Barrett SD, Bridges AJ, Dudley DT, Saltiel AR, Fergus JH, Flamme CM, et al. The discovery of the benzhydroxamate MEK inhibitors CI-1040 and PD 0325901. *Bioorg Med Chem Lett* 2008;18:6501–4.
30. Auersperg N, Wong AS, Choi KC, Kang SK, Leung PC. Ovarian surface epithelium: biology, endocrinology, and pathology. *Endocr Rev* 2001;22:255–88.
31. Feeley KM, Wells M. Precursor lesions of ovarian epithelial malignancy. *Histopathology* 2001;38:87–95.
32. Bowtell DD. The genesis and evolution of high-grade serous ovarian cancer. *Nat Rev Cancer* 2010;10:803–8.
33. NIH, Medicine NLo. Ovarian Cancer. Available at: <http://www.ncbi.nlm.nih.gov/medlineplus/ency/article/000889.htm>. 2010.
34. NCI.Cancer Topics: Ovarian Cancer. Available at: <http://www.cancer.gov/cancertopics/types/ovarian>. 2010.
35. Jemal A, Siegel R, Xu J, Ward E. Cancer statistics, 2010. *CA Cancer J Clin* 2010;60:277–300.
36. Bast RC Jr, Mills GB. Personalizing therapy for ovarian cancer: BRCA and beyond. *J Clin Oncol* 2010;28:3545–8.
37. Carpten JD, Faber AL, Horn C, Donoho GP, Briggs SL, Robbins CM, et al. A transforming mutation in the pleckstrin homology domain of AKT1 in cancer. *Nature* 2007;448:439–44.
38. Noske A, Kaszubiak A, Weichert W, Sers C, Niesporek S, Koch I, et al. Specific inhibition of AKT2 by RNA interference results in reduction of ovarian cancer cell proliferation: increased expression of AKT in advanced ovarian cancer. *Cancer Lett* 2007;246:190–200.
39. Orsulic S, Li Y, Soslow RA, Vitale-Cross LA, Gutkind JS, Varmus HE. Induction of ovarian cancer by defined multiple genetic changes in a mouse model system. *Cancer Cell* 2002;1:53–62.
40. Bleeker FE, Felicioni L, Buttitta F, Lamba S, Cardone L, Rodolfo M, et al. AKT1(E17K) in human solid tumours. *Oncogene* 2008;27:5648–50.
41. Davies MA, Stemke-Hale K, Tellez C, Calderone TL, Deng W, Prieto VG, et al. A novel AKT3 mutation in melanoma tumours and cell lines. *Br J Cancer* 2008;99:1265–8.
42. Ju X, Katiyar S, Wang C, Liu M, Jiao X, Li S, et al. Akt1 governs breast cancer progression in vivo. *Proc Natl Acad Sci U S A* 2007;104:7438–43.
43. Janakiraman M, Vakiani E, Zeng Z, Pratilas CA, Taylor BS, Chitale D, et al. Genomic and biological characterization of exon 4 KRAS mutations in human cancer. *Cancer Res* 2010;70:5901–11.
44. Pratilas CA, Hanrahan AJ, Halilovic E, Persaud Y, Soh J, Chitale D, et al. Genetic predictors of MEK dependence in non-small cell lung cancer. *Cancer Res* 2008;68:9375–83.
45. Venkatraman ES, Olshen AB. A faster circular binary segmentation algorithm for the analysis of array CGH data. *Bioinformatics* 2007;23:657–63.
46. TCGA. Comprehensive genomic characterization defines human glioblastoma genes and core pathways. *Nature* 2008;455:1061–8.
47. Nusse M, Beisker W, Hoffmann C, Tarnok A. Flow cytometric analysis of G1- and G2/M-phase subpopulations in mammalian cell nuclei using side scatter and DNA content measurements. *Cytometry* 1990;11:813–21.
48. Taylor BS, Schultz N, Hieronymus H, Gopalan A, Xiao Y, Carver BS, et al. Integrative genomic profiling of human prostate cancer. *Cancer Cell* 2010;18:11–22.
49. Tibes R, Qiu Y, Lu Y, Hennessy B, Andreeff M, Mills GB, et al. Reverse phase protein array: validation of a novel proteomic technology and utility for analysis of primary leukemia specimens and hematopoietic stem cells. *Mol Cancer Ther* 2006;5:2512–21.
50. Sakr RA, Barbashina V, Morrogh M, Chandraratnaty S, Andrade VP, Arroyo CD, et al. Protocol for PTEN expression by immunohistochemistry in formalin-fixed paraffin-embedded human breast carcinoma. *Appl Immunohistochem Mol Morphol* 2010;18:371–4.

Correction: Genomic Complexity and AKT Dependence in Serous Ovarian Cancer

In this article (*Cancer Discovery* 2012;2:56–67), which was published in the January 2012 issue of *Cancer Discovery* (2), the name of the 7th author is incorrect. The correct name is Manickam Janakiraman.

The authors regret this error.

REFERENCE

1. Hanrahan AJ, Schultz N, Westfal ML, Sakr RA, Giri DD, Scarperi S, et al. Genomic complexity and AKT dependence in serous ovarian cancer. *Cancer Discovery* 2012;2:56–67.

Published OnlineFirst March 9, 2012.

doi: 10.1158/2159-8290.CD-12-0075

©2012 American Association for Cancer Research.